

Multiple Kerf Quality Optimization in Laser Cutting of BFRP Composite using Grey Relational based Genetic Algorithm

Girish Dutt Gautam

Research Scholar
Department of Mechanical Engineering
Jaypee University of Engineering and
Technology, Guna-473226,
Madhya Pradesh
India

Dhananjay R. Mishra

Assistant professor (SG)
Department of Mechanical Engineering
Jaypee University of Engineering and
Technology, Guna-473226,
Madhya Pradesh
India

In laser beam machining, the geometrical precise cutting of fiber reinforced polymer (FRP) composite materials is a challenging task in order to produce a higher quality cut. The aim of the present research is to determine optimum levels of cutting parameters able to provide geometrically accurate cut for 1.60 mm thick Basalt Fiber Reinforced Polymer (BFRP) composite laminate. The total of 42 experiments have been performed on a 250W pulsed Nd:YAG laser system. During experimentation, the lamp current, pulse width, pulse frequency, compressed air pressure and cutting speed have been varied to evaluate different kerf quality characteristics such as top and bottom kerf width, top & bottom kerf deviation, and kerf taper. Experimental results have been used to single index optimization of evaluated multiple kerf quality characteristics. A hybrid grey relational analysis coupled with genetic algorithm approach has been adopted for the optimization. The optimum levels of cutting parameters have been found at moderate lamp current (184.5 Amp), lower pulse width (2 ms), compressed air pressure (8 kg/cm²) and cutting speed (50 mm/min) and higher pulse frequency (30 Hz). Finally, confirmation experiments have been conducted and it has been observed that optimal levels of cutting parameters are able to improve top kerf width, bottom kerf width, top kerf deviation, bottom kerf deviation, and kerf taper by 13.33 %, 13.29 %, 23.52 %, 23.07 %, and 10.83 %, respectively. From the experimental results, it has been found that lamp current is the most significant parameter for all kerf quality characteristics.

Keywords: Nd:YAG laser; Basalt fiber; Kerf characteristics; optimization; Grey relational analysis; Genetic algorithm.

1. INTRODUCTION

In recent decades, the interest of researchers focused on basalt fibers due to their higher mechanical performance and eco-friendly nature. These fibers are obtained from melted basalt rocks by an energy efficient extrusion process [1]. Silicon dioxide (SiO₂) and aluminium oxide (Al₂O₃) are the main constituents of basalt fibers. Superior thermal, electrical, abrasion, corrosion, and chemical resistant properties with higher shear and compression strength make basalt fibers and its composites suitable for a wide range of applications in automobile, aircraft, and manufacturing industries. Basalt fibers have a wide range of working temperature from -269 °C to 650 °C. Their composites are widely used for the production of car headliners, disc brake pads and clutch facing components, engine insulator due to their higher frictional, thermal and shock resistance properties in the automotive industries. Nowadays basalt fibers are increasingly replacing E-glass fibers and carbon fibers as a reinforcing agent of polymer matrix com-

posites due to its greater tensile and compressive properties and low cost. It has a similar chemical structure to the glass with slightly higher density and higher stability in an acidic environment. Basalt composite pipes are stronger as compare to glass fiber pipes for corrosive liquids and gases transportation [2].

In recent years, the applications of BFRP composites are increased in various engineering sectors. Machining of these composites is required for their structural applications. In their conventional machining, various frictional forces are developed and reduce their cut quality. Matrix cracking, thermal damages, whiskers formation, fiber losing and fiber delamination around cutting edges are some of the major drawbacks of conventional machining of BFRP composites. Advanced machining processes such as laser beam machining (LBM), water jet machining, plasma arc machining etc. compared to the conventional machining techniques provide superior cut quality during FRP composite machining. These processes also improve the production rate. [3].

Laser beam cutting (LBC) proves its wide acceptability for machining of FRP composites to obtain precise and complex profile cut. It provides a better cut quality and operation preciseness with low cost and improved machinability. In LBC, a high energy focused laser beam is utilized for removal of material from the work surface through melting and evaporation caused

Received: March 2020, Accepted: May 2020

Correspondence to: Dr Dhananjay R. Mishra, Mechanical Engineering Department, Jaypee University of Engineering and Technology, Guna-473226, India
E-mail: dm30680@gmail.com

doi:10.5937/fme2003636G

© Faculty of Mechanical Engineering, Belgrade. All rights reserved

FME Transactions (2020) 48, 636-650 636

by the thermal energy of beam [4]. As no cutting force is present in LBC, it offers minimal delamination and matrix cracking as compared to other machining techniques. This process is able to provide complex shapes with accurate geometries of cut edges with higher material removal rate for a wide range of materials such as metals, non-metals, ceramics and composites [5]. The geometry of the laser cut is defined in the terms of its kerf quality characteristics such as kerf width (KW), kerf deviation (KD) and kerf taper (KT). These parameters decide the quality, geometrical accuracy and precisions of the cut. Moreover, in laser cutting, a taper in cut edge geometry always exists due to the converging-diverging nature of laser beam and known as kerf taper [6-7].

Numerous researchers have analysed the effect of different laser cutting parameters on the different geometrical quality characteristics of the laser cut such as top and bottom kerf width, top and bottom kerf deviation and kerf taper for FRP composites. Mathew et al. [8] have been investigated the effect of cutting speed, pulse energy, pulse duration, pulse repetition rate and gas pressure on the top and bottom kerf widths, kerf taper and heat affected zone in pulsed Nd:YAG laser cutting of carbon fiber reinforced plastic (CFRP) composites. They observed that pulse repetition rate and pulse energy were the most influencing factors for the kerf widths. They also found that at high cutting speed a no cut-situation is observed. Negarestani et al. [9] employed a nano-second pulsed DPSS Nd:YAG laser for cutting of CFRP composites to investigate the kerf taper and material removal rate with using mixed reactive and inert gases. They observed that higher cut quality can be achieved through the use of low oxygen content assistant gas. Leone and Genna [10] used a 150W Nd:YAG pulsed laser for cutting of CFRP composite. They observed that an accurate selection of the laser cutting parameters can reduce heat affected zone (HAZ) and KT. Cenna and Mathew [11] developed a model based on energy balance equations to predict kerf width and kerf taper angle during laser cutting of glass fiber reinforced polymer (GFRP) and aramid fiber reinforced polymer (AFRP) composite samples of varying thickness. They have revealed that for both materials average kerf angle decreases with increasing cutting speed.

Gautam and Pandey [12] evaluated the effects of different laser cutting parameters such as lamp current, pulse width, pulse frequency, compressed air pressure and cutting speed on top and bottom kerf deviation in Nd:YAG laser cutting of AFRP composite. They found that the lamp current is the highest affecting factor for both the top kerf deviation and bottom kerf deviation followed by pulse frequency.

In the detailed literature survey, limited research work is found for laser cutting of BFRP composites as individual or ingredient of hybrid laminates. Gautam and Mishra [13] performed the laser cutting of 1.60 mm thick Basalt fiber based composite sheet. They also employed firefly based multiobjective optimization approach to optimize kerf width, kerf deviation and kerf taper. They observed that lamp current influenced the kerf width and kerf taper remarkably. They also found

that pulse frequency has negligible effects on all kerf quality characteristics. In another study, Gautam and Mishra [14] performed the laser cutting of 1.35 mm thick Kevlar-29 and Basalt fiber based hybrid composite sheet. They observed that the geometrical accuracy of the cut not only affected by the laser cutting parameters but also by the specific properties of Kevlar-29 and basalt fibers with epoxy resin. In another study [15], they observed that lower lamp current, pulse frequency and compressed air pressure whereas higher cutting speed is required for dimensionally accurate laser cutting of Kevlar-29 and Basalt fiber based hybrid composite sheet.

In LBC, it has been observed that achieving a better cut quality is a tough task due to the nonlinear relationship between the input and output parameters. To overcome this problem, various researchers employed different optimization techniques to obtain optimum levels of laser cutting parameters for achieving higher cut quality. El-taweel et al. [16] used Taguchi methodology (TM) to find optimum laser cutting parameters such as laser power, cutting speed, assistance gas pressure and laser mode setting to minimize kerf width, dross height, and slope of the cut for KFRP composite. Choudhury and Chuan [17] found significant improvement in kerf width and surface roughness using optimal settings of cutting parameters such as nozzle diameter, material thickness and cutting speed in CO₂ laser cutting of GRRP by using response surface methodology (RSM). They observed that better surface finish and kerf width achieved at small nozzle diameter.

In multi-objective optimization problems, weight factor determination for each quality characteristic is the key issue. Grey relational analysis provides an efficient solution for the simultaneous optimization of multiple quality characteristics containing discrete data. GRA proves its suitability in various field of engineering such as manufacturing, economic and management systems [18].

Adalarasan et al. [19] employed a hybrid approach of grey based response surface methodology (GRSM) for predicting the optimal combination of laser cutting parameters such as laser power, pulsing frequency, cutting speed and assist gas pressure for improved kerf width, surface finish and cut edge slope in CO₂ laser cutting of metal matrix composites. They observed a substantial improvement in the cut quality characteristics by employed hybrid technique. Rao and Yadava [20] employed a hybrid approach of TM and GRA to minimize the kerf width, kerf taper, and kerf deviation together during pulsed Nd:YAG laser cutting of a nickel -based super alloy. They considered oxygen pressure, pulse width, pulse frequency, and cutting speed as process parameters. They observed that the employed approach improved all kerf quality characteristics remarkably.

Tamrin et al. [21] used GRA to obtain a single optimal set of laser cutting parameters such as laser power, cutting speed and compressed air pressure for minimal HAZ and cut diameter in three different thermoplastics such as poly-methyl-methacrylate, polycarbonate and polypropylene. Mishra et al. [22] employed GRA technique for single index optimization of top and bottom kerf deviations during pulsed Nd:YAG

laser cutting of a novel 2.34 mm thick Kevlar-29, Basalt and Glass fiber based hybrid FRP composite laminate. In recent years, GRA is successfully coupled with genetic algorithm by some researchers. They observed that hybrid GRA is able to improve optimum results significantly compared with alone GRA [23].

In a detailed literature survey, it is observed that the potential of laser beam machining for BFRP composites is yet to be explored. An optimum set of laser cutting parameters are also essential for the economic and competent cutting. Keeping this fact in mind, a detailed parametric study has been conducted to investigate the effects of five different laser cutting parameters like lamp current (I), pulse width (PW), pulse frequency (f), compressed air pressure (p) and cutting speed (S) on multiple kerf quality characteristics viz. top kerf width (TKW), bottom kerf width (BKW), top kerf deviation (TKD), bottom kerf deviation (BKD) and kerf taper (KT) in pulsed Nd:YAG laser beam cutting of BFRP composite laminate. A grey relational analysis based genetic algorithm (GRGA) optimization technique has been applied to optimize multiple kerf quality characteristics as a single performance index. Finally, a confirmation test has been carried out to validate the optimum results obtained by the employed approach. The paper also discusses the effect of significant control factors on the multiple kerf quality characteristics.

2. EXPERIMENTAL PROCEDURE

2.1 Material & Experimental Set-up

In the present research, BFRP composite laminate has been used as workpiece material. In this composite, basalt fiber has been used as the reinforcing agent in the epoxy-based matrix phase. The woven mat of Basalt fibers was supplied by Aerotech Technical Textile, Mumbai, India having thickness 200 gsm. Moreover,

epoxy resin-520 and hardner-509 have been used as a polymeric binding agent, manufactured by Electro coating & Insulation Technical Pvt. Ltd., Pune, India. Table 1 and 2 contain the properties of employed woven basalt fabric, epoxy resin-520 and hardener-509 respectively.

The 1.60 mm thick BFRP composite laminate has been fabricated by using the hand-layup technique in the ideal laboratory environment. In the fabrication process of BFRP composite laminates, a mild steel mold having dimensions 300 mm×300 mm×20 mm is used. In the literature survey, it has been observed that the physical properties of the laminate depend on the matrix impregnation and the orientation of the fibers. Therefore, the orientations of basalt fiber mats in fabricated laminates have been kept [B-0°/B-90°/B-0°/B-90°/B-0°/B-90°/B-0°] for the seven layers. The orientation angle of (0°/90°), has been taken for the better flow of the matrix because epoxy needs a larger space to flow. The dimensions of the fabricated laminate were 150 mm×250 mm×1.60 mm. The volume and weight fraction for fiber 87.50 % and 12.50 % and for matrix as 78.75 % and 21.25 %, found in fabricated laminate. Moreover, theoretical density of the BFRP laminate was observed 0.60 g/cm³. These physical properties ensure the higher mechanical properties of the laminate because of holding higher fiber volume. The process for BFRP composite fabrication is shown in Fig. 1.

The cutting experiments for BFRP composite laminate are performed by a pulsed Nd:YAG laser beam machine developed at Raja Rammana Center of Advanced Technology (RRCAT), Indore, India, having 250W average output power and a three axes CNC-controlled table using compressed air as the assist gas. The impact angle between the laser beam and composite surface kept 90° throughout the experimentation process. Stand-off distance also fixed at 1 mm during experimentation.

Table 1. Properties of basalt fiber fabric

Fiber Species (textile)		Size (mm)		Area weight (g/m ²)
Warp	Welt	Width	thickness	
80	80	100-1500	0.20	160

Table 2. Properties of epoxy resin and hardener

Properties	Unit	Epoxy resin-520	Hardener -509
Color and appearance	-	Colorless/clear liquid	Clear yellow to haze
Viscosity at 27°C	MPa.s	7000-14000	60-80
Density at 27°C	g/cc	1.05-1.150	-
Epoxy equivalent	g/equivalent	180-210	-

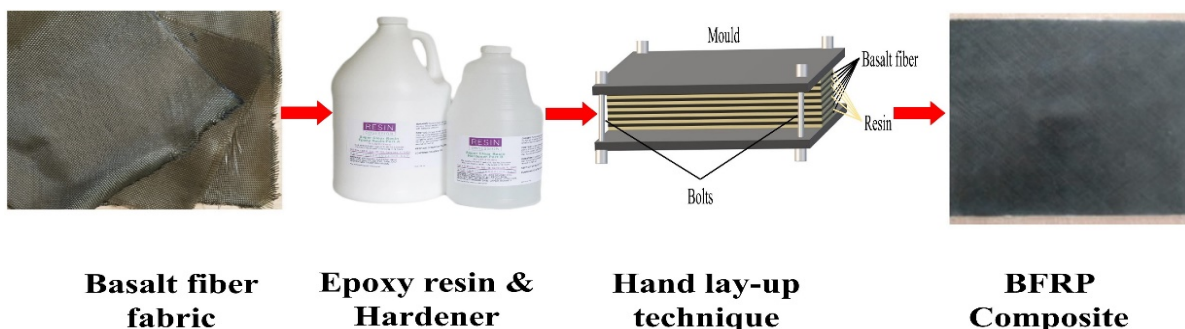


Figure 1. BFRP composite laminate fabrication process

2.2 Design of experiments

In the literature survey, it has been observed that the kerf quality characteristics of the cut surface depend on the leading laser machining parameters such as lamp current (I), pulse width (PW), pulse frequency (f), compressed air pressure (p) and cutting speed (S). A range of pilot experiments has been performed to minimize the suitable range of laser cutting parameters. Pilot experiments also help to define the lower and higher tolerable ranges of parameters for acceptable cut quality. In this research, the experiments have been designed according to the box-behnken design based on the response surface methodology. The box-behnken design is selected due to fewer design points as compared to full factorial design and central composite design with avoiding an extreme combination of factors. Five variable laser cutting parameters (I , PW , f , p and S) with three levels of each have been used to conduct forty-two experiments. The levels of the laser cutting parameters are shown in Table 3.

Table 3. Laser cutting parameters and levels

Factor	Unit	Levels		
Lamp current	Amp	180	200	220
Pulse width	ms	2	2.5	3
Standoff distance	mm	1	1.5	2
Air Pressure	kg/cm ²	8	10	12
Cutting speed	mm/min	100	150	200

2.3 Kerf quality characteristics

For each combination of cutting parameters, a 30 mm long straight cut has been performed to ascertain kerf quality characteristics. The kerf width indicates the loss of material in cut and kerf deviation represents the waviness of kerf, while kerf taper shows the difference in the top kerf width and bottom kerf width of the cut.

The measurement of the kerf width has been performed by a stereo optical microscope with a maximum magnification capacity of 160X. Six KW's

(viz. K_1 , K_2 , K_3 , K_4 , K_5 , and K_6) have been measured on both top and bottom side of the cut. The average values of kerf are acquired in each cut for analysis. Equation 1, 2, 3, 4 and 5 have been used to calculate values of TKW, BKW, TKD, BKD, and KT, respectively.

$$TKW = \frac{(K_1 + K_2 + K_3 + K_4 + K_5 + K_6)_{Top\ side}}{6} \quad (1)$$

$$BKW = \frac{(K_1 + K_2 + K_3 + K_4 + K_5 + K_6)_{Bottom\ side}}{6} \quad (2)$$

$$TKD = Maximum\ TKW - Minimum\ TKW \quad (3)$$

$$BKD = Maximum\ BKW - Minimum\ BKW \quad (4)$$

$$KT = \frac{(TKW - BKW) \times 180}{2\pi t} \quad (5)$$

where, t is the thickness of the BFRP composite laminate. Figure 2 shows the complete process of experimentation and measurement. The variation of measured values of TKW and BKW and calculated values of TKD and BKD, and KT are shown in Fig. 3, 4 and 5, respectively.

3. GREY RELATIONAL BASED GENETIC ALGORITHM (GRGA) OPTIMIZATION TECHNIQUE

The Grey relational based genetic algorithm (GRGA) optimization technique contains two established optimization approaches i.e. grey relational analysis (GRA) and genetic algorithm (GA). In this approach, GRA is used to identify relationships between process parameters and output responses [14, 22-23]. Calculated grey relational grades considered as a single performance quality index for all responses. A second-order regression mathematical model is developed by using calculated grey relational grade. This model is used as an objective function for GA based optimization process. The technique of GRGA is disclosed in two phases as shown in Fig. 6.

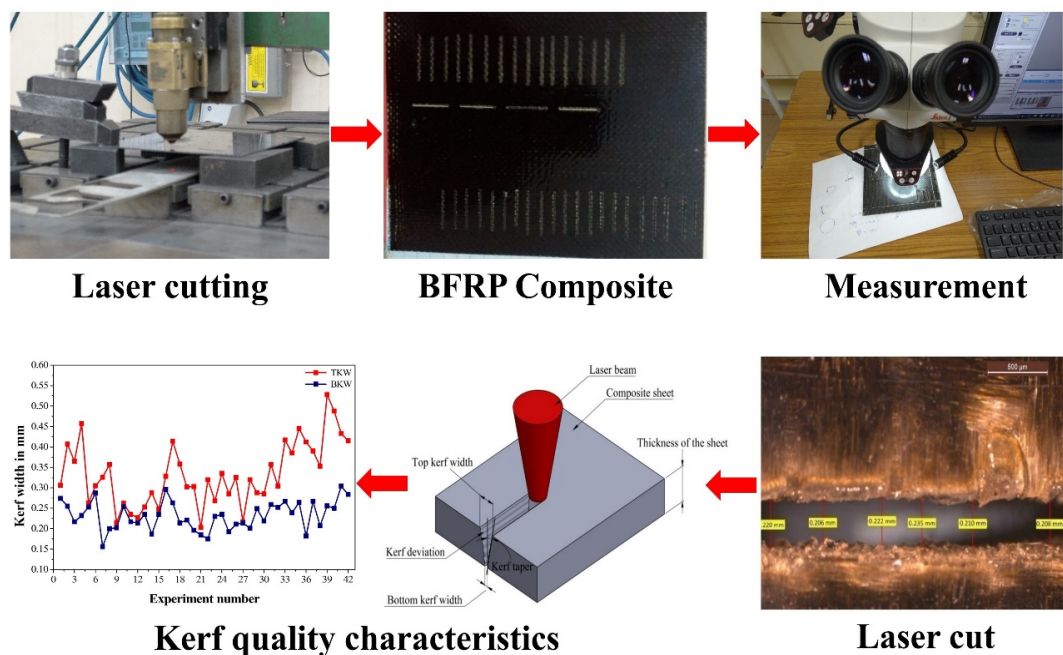


Figure 2. Process diagram of experimentation and measurement

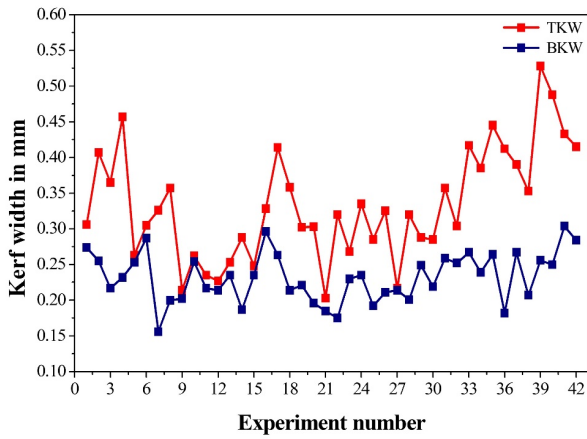


Figure 3. Variation of TKW and BKW for all experiments

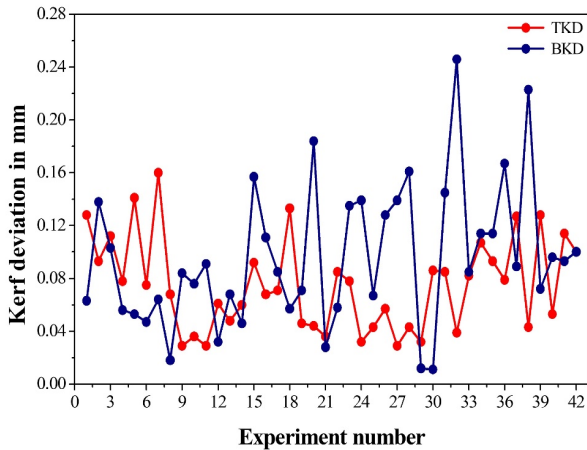


Figure 4. Variation of TKD and BKD for all experiments

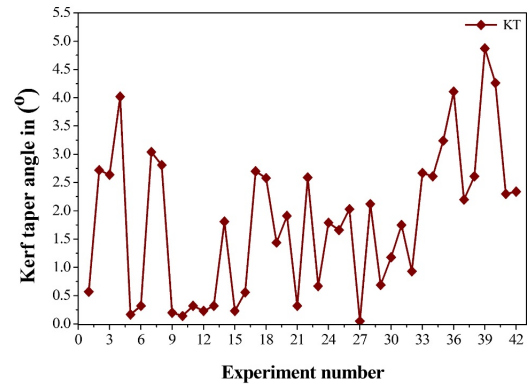


Figure 5. Variation of KT for all experiments

Grey relational analysis was introduced by Prof. Deng in 1982. He found that GRA is able to provide a decision about the system containing incomplete or complete information. GRA offers competent solution to the uncertain and discrete data system. It provides interrelationship between the process parameters and performance characteristics based on grey system theory. In GRA, the system information is determined by black and white color. No information situation of a system is represented by the black color. While white color represents a system having some information. The information level between black and white denotes by grey color. In other words, in a grey system, part information about the system is certain and part information is uncertain or unknown. So, grey system provides some certain and some uncertain relationships among the factors in a system. GRA is a measurement process of the absolute value of the data variance between sequences, and it ensures the approximate correlation between sequences.

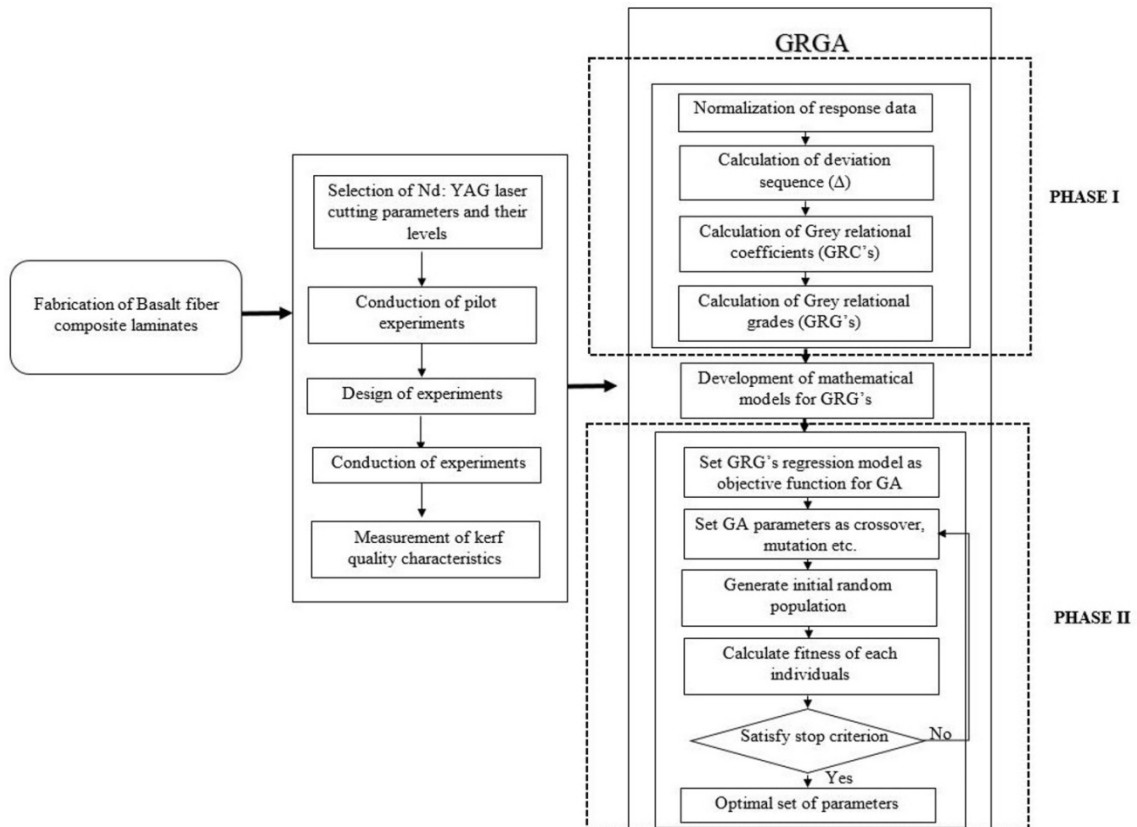


Figure 6. Methodology of GRGA approach

In GRA, grey relational generating is the first step to pre-processing of the entire range of data. Grey relational generating is necessary to develop a comparable sequence of original scatter data sequence. Thus, in grey relational generating, scatter data is transformed into normalized, scaled and polarized form in the range between 0 and 1. Three equations are used for normalization process shown in Eq. 6, 7 and 8 i.e. larger-the better, nominal is best and smaller-the better.

$$Z_{ij} = \frac{Y_{ij} - \min(Y_{ij})}{\max(Y_{ij}) - \min(Y_{ij})} \quad (\text{Larger-the better}) \quad (6)$$

$$Z_{ij} = 1 - \frac{|Y_{ij} - Y_i|}{\max(Y_{ij}) - Y_i} \quad (\text{Nominal is best}) \quad (7)$$

$$Z_{ij} = \frac{\max(Y_{ij}) - Y_{ij}}{\max(Y_{ij}) - \min(Y_{ij})} \quad (\text{Smaller-the better}) \quad (8)$$

where, Z_{ij} is the normalized value for i^{th} experiment for j^{th} response, Y_i is the i^{th} normalized value and Y_{ij} is the i^{th} normalized value for j^{th} response.

Equation 8 is used for the normalization process in this research because all five kerf quality characteristics (viz. TKW, BKW, TKD, BKD, and KT) are the smaller-the better quality characteristics. Then, grey relational coefficients (GRC's) are calculated by using Eq. 9.

$$Z_{ij} = \frac{\max(Y_{ij}) - Y_{ij}}{\max(Y_{ij}) - \min(Y_{ij})} \quad (9)$$

where, GC_{ij} is the grey relational coefficient for the i^{th} experiment and j^{th} response. Δ is the absolute difference between Y_{oj} and Y_{ij} ; here Y_{oj} is the ideal normalized value of j^{th} response. Δ_{\min} and Δ_{\max} are the minimum and maximum values of Δ , respectively. λ is the distinguishing coefficient having range $0 \leq \lambda \leq 1$. In this study, the value of λ is taken as 0.5. Δ_{\min} and Δ_{\max} are calculated by Eq. 10 and 11.

$$\Delta_{\min} = \left(\min_{\forall j \in i} \right) \left(\max_{\forall j \in i} \right) \|Y_{oj} - Y_{ij}\| \quad (10)$$

$$\Delta_{\max} = \left(\max_{\forall j \in i} \right) \left(\max_{\forall j \in i} \right) \|Y_{oj} - Y_{ij}\| \quad (11)$$

Weighting ratio 1:1:1:1:1 has been set for all five kerf quality characteristics for incorporating the GRC's into the grey relational grade for each experiment. Grey relational grades (G_i) were computed as per Eq. 12.

$$G_i = \frac{1}{m} \sum GC_{ij} \quad (12)$$

where, m is the number of responses.

Then, the mathematical model of the calculated Grey relation grades is used as an objective function for Genetic Algorithm (GA). It is one of the most popular evolutionary approaches for the optimization of the linear and the nonlinear complex problems. GA is able to identify the global optimum point without the limitation of the gradient methods. GA is based on

Darwin's principle of natural selection (i.e. survival of the fittest).

The working of GA starts with a population of initial solutions generated at random. Then, the fitness /goodness value of the objective function is calculated in the case of a maximization problem. If the objective function has a minimization problem then it is converted into a corresponding maximization problem. Thereafter, the population of solutions is modified by using different operators namely reproduction, crossover, mutation and others. It is considered that all the solutions in a population may not be equally good in terms of their fitness values. Therefore, an operator named reproduction is utilized to select good solutions using their fitness values. It forms a mating pool consisting of good solutions probabilistically. The mating pool can contain multiple copies of the particular good solution.

The size of the mating pool is kept equal to the population of solutions considered before reproduction. Thus, the average fitness of the mating pool is expected to be higher than the pre-reproduction population of solutions. The proportionate selection (Roulette-Wheel selection), tournament selection, ranking selection are various types of reproduction schemes. The mating pairs or the parents are selected randomly from the mating pool.

The mating pair participates in the crossover which depends upon the value of crossover probability. The properties between the parents and new children are exchanged in the crossover stage and mutation is occurred. It is considered that if the parents are good, the children are expected to be good. Mutation represents the sudden change of a parameter or improvement in the gene of the child. In a GA search, the mutation is required to achieve a local change around the current solution and shift it to the global solution. After the reproduction, crossover and mutation are applied to the whole population of solutions. This whole process represents the one generation of GA [27]. This process is repeated until to achieve the best fitness values of function.

4. RESULTS AND DISCUSSION

4.1 GRGA based multiobjective optimization

GRA has been applied to transform scatter data in the normalized form to obtain relationships between laser cutting parameters and kerf quality characteristics. All kerf quality characteristics are considered as smaller-the better characteristics.

Equation 8 has been used to perform linear normalization of all five kerf quality characteristics. Table 4 shows the normalized values and deviational sequence for TKW, BKW, TKD, BKD, and KT. Calculated GRC's and GRG's for all responses with their ranks are shown in Table 5. The values of Grey relational grade show a single representation for all kerf quality characteristics for a combination of cutting parameters. The highest value of GRG has been observed at the twenty-one experimental run as 0.8783.

Table 4. The calculated normalized values and deviation sequences

Exp. No.	Normalized values					Deviational sequence				
	TKW	BKW	TKD	BKD	KT	Δ_1	Δ_2	Δ_3	Δ_4	Δ_5
1	0.6830	0.2027	0.2442	0.7787	0.8902	0.3169	0.7972	0.7557	0.2212	0.1097
2	0.3723	0.3310	0.5114	0.4595	0.4451	0.6276	0.6689	0.4885	0.5404	0.5548
3	0.5015	0.5878	0.3664	0.6085	0.4616	0.4984	0.4121	0.6335	0.3914	0.5383
4	0.2184	0.4864	0.6259	0.8085	0.1759	0.7815	0.5135	0.3740	0.1914	0.8240
5	0.8153	0.3445	0.1450	0.8212	0.9730	0.1846	0.6554	0.8549	0.1787	0.0269
6	0.6861	0.1148	0.6488	0.8468	0.9420	0.3138	0.8851	0.3511	0.1531	0.0579
7	0.6215	1.0000	0.0000	0.7744	0.3788	0.3784	0.0000	1.0000	0.2255	0.6211
8	0.5261	0.7027	0.7022	0.9702	0.4265	0.4738	0.2972	0.2977	0.0297	0.5734
9	0.9661	0.6891	1.0000	0.6893	0.9668	0.0338	0.3108	0.0000	0.3106	0.0331
10	0.8184	0.3378	0.9465	0.7234	0.9792	0.1815	0.6621	0.0534	0.2765	0.0207
11	0.9015	0.5878	1.0000	0.6595	0.9420	0.0984	0.4121	0.0000	0.3404	0.0577
12	0.9261	0.6081	0.7557	0.9106	0.9606	0.0738	0.3918	0.2442	0.0893	0.0393
13	0.8461	0.4662	0.8549	0.7574	0.9420	0.1538	0.5337	0.1450	0.2425	0.0579
14	0.7384	0.7905	0.7633	0.8510	0.6335	0.2615	0.2094	0.2366	0.1489	0.3664
15	0.8615	0.4662	0.5190	0.3787	0.9606	0.1384	0.5337	0.4809	0.6212	0.0393
16	0.6153	0.0540	0.7022	0.5744	0.8923	0.3846	0.9459	0.2977	0.4255	0.1076
17	0.3507	0.2770	0.6793	0.6851	0.4492	0.6492	0.7229	0.3206	0.3148	0.5507
18	0.5230	0.6081	0.2061	0.8042	0.4741	0.4769	0.3918	0.7938	0.1957	0.5258
19	0.6953	0.5608	0.8702	0.7446	0.7101	0.3046	0.4391	0.1297	0.2553	0.2898
20	0.6923	0.7297	0.8854	0.2638	0.6128	0.3076	0.2702	0.1145	0.7361	0.3871
21	1.0000	0.8040	0.9465	0.9276	0.9420	0.0000	0.1959	0.0534	0.0723	0.0579
22	0.6400	0.8716	0.5725	0.8000	0.4720	0.3600	0.1283	0.4274	0.2000	0.5279
23	0.8000	0.5000	0.6259	0.4723	0.8695	0.2000	0.5000	0.3740	0.5276	0.1304
24	0.5938	0.4662	0.9770	0.4553	0.6376	0.4061	0.5337	0.0229	0.5446	0.3623
25	0.7476	0.7567	0.8931	0.7617	0.6645	0.2523	0.2432	0.1068	0.2382	0.3354
26	0.6246	0.6283	0.7862	0.5021	0.5879	0.3753	0.3716	0.2137	0.4978	0.4120
27	0.9569	0.6081	1.0000	0.4553	0.9979	0.0430	0.3918	0.0000	0.5446	0.0020
28	0.6400	0.6959	0.8931	0.3617	0.5693	0.3600	0.3040	0.1068	0.6382	0.4306
29	0.7384	0.3716	0.9770	0.9957	0.8654	0.2615	0.6283	0.0229	0.0042	0.1345
30	0.7476	0.5743	0.5648	1.0000	0.7639	0.2523	0.4256	0.4351	0.0000	0.2360
31	0.5261	0.3040	0.5725	0.4297	0.6459	0.4738	0.6959	0.4274	0.5702	0.3540
32	0.6892	0.3513	0.9236	0.0000	0.8157	0.3107	0.6486	0.0763	1.0000	0.1842
33	0.3415	0.2500	0.5954	0.6851	0.4554	0.6584	0.7500	0.4045	0.3148	0.5445
34	0.4400	0.4391	0.4045	0.5617	0.4679	0.5600	0.5608	0.5954	0.4382	0.5320
35	0.2553	0.2702	0.5114	0.5617	0.3374	0.7446	0.7297	0.4885	0.4382	0.6625
36	0.3569	0.8243	0.6183	0.3361	0.1573	0.6430	0.1756	0.3816	0.6638	0.8426
37	0.4246	0.2500	0.2519	0.6680	0.5527	0.5753	0.7500	0.7480	0.3319	0.4472
38	0.5384	0.6554	0.8931	0.0978	0.4679	0.4615	0.3445	0.1068	0.9021	0.5320
39	0.0000	0.3243	0.2442	0.7404	0.0000	1.0000	0.6756	0.7557	0.2595	1.0000
40	0.1230	0.3648	0.8167	0.6382	0.1262	0.8769	0.6351	0.1832	0.3617	0.8737
41	0.2923	0.0000	0.3511	0.6510	0.5320	0.7076	1.0000	0.6488	0.3489	0.4679
42	0.3476	0.1351	0.4580	0.6212	0.5238	0.6523	0.8648	0.5419	0.3787	0.4761

Table 5. The calculated grey relational coefficients and grey relational grades

Exp. No.	GRC					GRG	Rank
	TKW	BKW	TKD	BKD	KT		
1	0.6120	0.3854	0.3981	0.6932	0.8200	0.5817	24
2	0.4433	0.4277	0.5057	0.4805	0.4739	0.4662	39
3	0.5007	0.5481	0.4410	0.5608	0.4815	0.5064	32
4	0.3901	0.4933	0.5720	0.7230	0.3776	0.5112	29
5	0.7303	0.4327	0.3690	0.7366	0.9489	0.6435	14
6	0.6143	0.3609	0.5874	0.7654	0.8961	0.6448	13
7	0.5691	1.0000	0.3333	0.6891	0.4459	0.6075	21
8	0.5134	0.6271	0.6267	0.9437	0.4657	0.6353	15
9	0.9365	0.6166	1.0000	0.6167	0.9378	0.8215	2
10	0.7336	0.4302	0.9034	0.6438	0.9602	0.7342	7
11	0.8354	0.5481	1.0000	0.5949	0.8961	0.7749	5
12	0.8713	0.5606	0.6717	0.8483	0.9270	0.7758	4
13	0.7647	0.4836	0.7751	0.6733	0.8961	0.7185	8
14	0.6565	0.7047	0.6787	0.7704	0.5770	0.6775	11
15	0.7831	0.4836	0.5097	0.4459	0.9270	0.6299	16
16	0.5652	0.3457	0.6267	0.5402	0.8228	0.5801	25

17	0.4350	0.4088	0.6093	0.6135	0.4758	0.5085	31
18	0.5118	0.5606	0.3864	0.7186	0.4873	0.5329	28
19	0.6214	0.5323	0.7939	0.6619	0.6330	0.6485	12
20	0.6190	0.6491	0.8136	0.4044	0.5635	0.6099	20
21	1.0000	0.7184	0.9034	0.8736	0.8961	0.8783	1
22	0.5813	0.7956	0.5390	0.7142	0.4864	0.6233	17
23	0.7142	0.5000	0.5720	0.4865	0.7931	0.6131	18
24	0.5517	0.4836	0.9562	0.4786	0.5798	0.6100	19
25	0.6646	0.6727	0.8238	0.6772	0.5985	0.6873	9
26	0.5711	0.5736	0.7005	0.5010	0.5482	0.5789	26
27	0.9206	0.5606	1.0000	0.4786	0.9958	0.7911	3
28	0.5813	0.6218	0.8238	0.4392	0.5372	0.6007	22
29	0.6565	0.4431	0.9562	0.9915	0.7879	0.7670	6
30	0.6646	0.5401	0.5346	1.0000	0.6793	0.6837	10
31	0.5134	0.4180	0.5390	0.4671	0.5854	0.5046	33
32	0.6166	0.4352	0.8675	0.3333	0.7307	0.5967	23
33	0.4316	0.4000	0.5527	0.6135	0.4786	0.4953	35
34	0.4716	0.4713	0.4564	0.5328	0.4844	0.4833	36
35	0.4017	0.4065	0.5057	0.5328	0.4300	0.4554	41
36	0.4374	0.7400	0.5671	0.4296	0.3723	0.5093	30
37	0.4649	0.4000	0.4006	0.6010	0.5278	0.4788	37
38	0.5200	0.5920	0.8238	0.3566	0.4844	0.5553	27
39	0.3333	0.4252	0.3981	0.6582	0.3333	0.4296	42
40	0.3631	0.4404	0.7318	0.5802	0.3639	0.4959	34
41	0.4140	0.3333	0.4352	0.5889	0.5165	0.4576	40
42	0.4339	0.3663	0.4798	0.5690	0.5121	0.4722	38

Table 6. Response means for grey relational grades

Laser parameters	Average grey relational grade by factor level				
	Level 1	Level 2	Level 3	Max-Min	Rank
<i>I</i>	0.5746	0.6569*	0.4818	0.1752	1
<i>PW</i>	0.5874	0.6030	0.6413*	0.0539	4
<i>F</i>	0.6232	0.5804	0.6723*	0.0919	3
<i>P</i>	0.7028*	0.5822	0.5870	0.1205	2
<i>S</i>	0.6256*	0.6006	0.6069	0.0250	5

*Optimum setting

The response means of calculated grey relational grades are shown in Table 6. By response means, it has been found that the optimal combination of laser cutting parameters is at lower levels of compressed air pressure and cutting speed, and a moderate level of lamp current and higher levels of pulse width and pulse frequency. At these levels, the values of cutting parameters are lamp current at 180 Amp, pulse width at 2.6 ms, pulse frequency at 30 Hz, compressed air pressure at 8 kg/cm² and cutting speed at 50 mm/min. It has been observed in the analysis that grey relational grades are highly influenced by lamp current followed by compressed air pressure, pulse frequency, pulse width and cutting speed.

After calculating grey relational grades for all the experimental trials, a second-order regression model has been developed and shown in Eq. 13.

$$\begin{aligned}
 GRG = & 7.18 + 0.0662I - 1.20PW + 0.0142f \\
 & - 2.440p - 0.00266S - 0.000143I * I \\
 & + 0.51PW * PW + 0.004f * f + 0.09p * p \\
 & + 0.00001S * S - 0.006I * PW - 0.0009I * f \\
 & + 0.0005I * p - 0.00005I * S - 0.08PW * f \\
 & + 0.22PW * p + 0.001PW * S + 0.0006f * p \\
 & - 0.00013f * S + 0.000915p * S
 \end{aligned} \tag{13}$$

In the present work, the accuracy and adequacy of the developed mathematical model of grey relational grades have been decided by using the surface and contour plots of the standard error of design as shown in Fig. 7.

The circular shape of these plots demonstrates that the developed model has a better degree of fitness. This is due to the uniform trend of the standard error of design with respect to control parameters. The degree of fitness shows that the sample data of the developed model follows the normal distribution.

Basically, it determines whether the sets of observed data match the expected outcomes through the applicable model. The analysis of variance (ANOVA) has been performed to determine the fitness and adequacy of the developed quadratic model. The S-value and coefficient of determination (R² and adjusted-R²) values of the developed model have been found as 0.0477513, 90.76 % and 81.96 %, respectively. These values show that the developed model is adequate and significant for data prediction. From the ANOVA table, it has been found that F-value and P-value of developed model are in the acceptable range and confirm the adequacy of the model.

The developed mathematical model as shown in Eq. 13 has been used as an objective function to minimize

TKW, BKW, TKD, BKD and KT for GA based optimization. Before the execution of GA, its control parameters have been defined such as population size, crossover probability, and mutation probability etc. Then an initial random population has been generated by employing MATLAB M-files coding. In the present research work, initial population size has been considered as 50. Two points based crossover function having a crossover probability of 0.8 with uniform mutation function and mutation probability of 0.01 are chosen for GA operator's values. Initially, the generation limit has been set to 300.

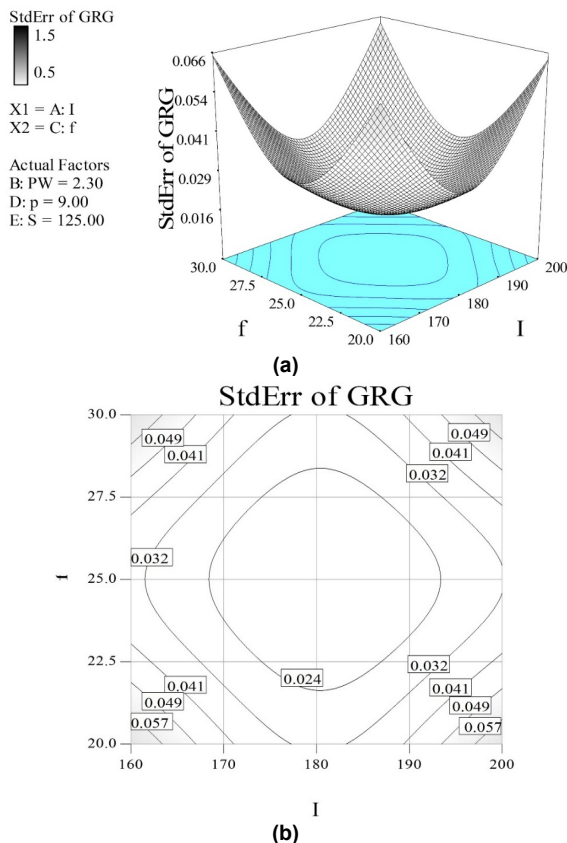


Figure 7. Variation of standard error for GRGs with respect to lamp current and pulse frequency (a) Surface plot (b) Contour plot

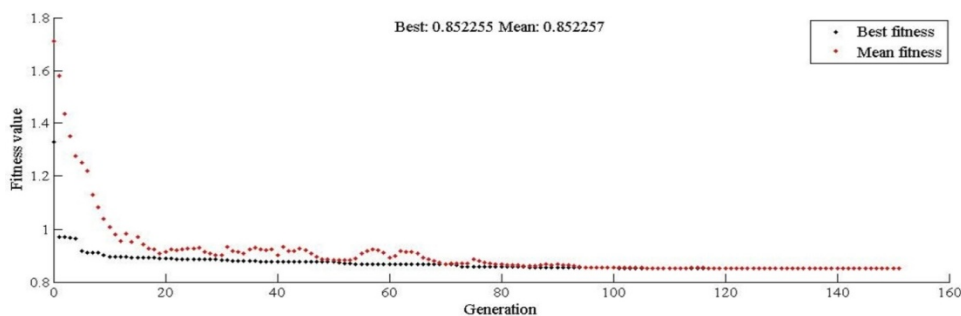


Figure 8. Variation of fitness values of the objective function with generations

Table 6. Results of confirmation experiments

S. No.	Kerf quality characteristics	GRA technique		GRGA technique		% Improvement
		Optimum setting	Experimental values	Optimum Setting	Experimental values	
1	TKW	$I=180$ Amp; $PW=2.6$ ms; $f=30$ Hz; $p=8$ kg/cm ² ; $S=50$ mm/min;	0.165	$I=184.5$ Amp; $PW=2$ ms; $f=30$ Hz; $p=8$ kg/cm ² ; $S=50$ mm/min;	0.143	13.33
2	BKW		0.158		0.137	13.29
3	TKD		0.034		0.026	23.52
4	BKD		0.013		0.010	23.07
5	KT		0.120		0.107	10.83

Then, the optimum values of process parameters have been selected based on the best fitness value. During the execution of GA, a lower bound [160, 2, 20, 8, 50] and an upper bound [200, 2.6, 30, 10, 200] have been used for five laser cutting parameters as lamp current, pulse width, pulse frequency, compressed air pressure and cutting speed, respectively. The best fitness value for the desired objective function is achieved after 151 generations, shown in Fig. 8. The values of the best fitness and mean fitness have been found at 0.852255 and 0.852257, respectively. The optimal values of different laser cutting parameters have been found by using GRGA approach as lamp current at 184.508 Amp, pulse width at 2 ms, pulse frequency at 30 Hz, compressed air pressure at 8 kg/cm² and cutting speed at 50 mm/min respectively.

4.2 Experimental validation

Experimental validation of optimal solutions has been performed by using optimal settings obtained by both GRA and hybrid GRGA approach. As mentioned in the previous section, the optimal solutions achieved by using GRA and GRGA technique are as $I=180$ Amp; $PW=2.6$ ms, $f=30$ Hz, $p=8$ kg/cm² and $S=50$ mm/min and $I=184.5$ Amp; $PW=2$ ms; $f=30$ Hz; $p=8$ kg/cm²; and $S=50$ mm/min respectively.

The aim of these optimal solutions is to minimize TKW, BKW, TKD, BKD, and KT. The results of the confirmation test for TKW, BKW, TKD, BKD, and KT are tabulated in Table 7. It has been found that GRGA approach significantly improved the kerf quality characteristics as compared to optimal settings of parameters obtained by GRA. An improvement of 13.33 %, 13.29 %, 23.52 %, 23.07 %, and 10.83 % has been observed in TKW, BKW, TKD, BKD, and KT, respectively with the GRGA setting against GRA optimal parameter settings. It has been observed that GRGA provides an overall improvement of 16.80 % for all kerf characteristics as compared to GRA. The maximum improvement is observed in TKD followed by the BKD, TKW, BKW, and KT.

4.3 Parametric effects analysis

The effect of different pulsed Nd:YAG laser cutting parameters on the multiple kerf quality characteristics in a single performance index represented by GRG during machining of BFRP composite laminates have been analysed by surface and contour plots. Figures 9-12 visually depicts the combined effects of I - PW , I - f , I - p and I - S on the values of the grey relational grades. From Fig. 9-12, it has been revealed that an increase in the value of lamp from 160 to 180 Amp, steps up the values of grey relational grades. However, the values of grey relational grades are decreased in the further increase in lamp current from 180 to 200 Amp. This may be due to that a higher lamp current increase the energy absorption tendency of BFRP composite surface through the incident laser beam. Whereas, basalt fiber has higher heat resistant properties so higher energy is required to smooth and higher cut quality. Moreover, higher lamp current (200 Amp) also increase the rate of vaporization of epoxy resin and affect the geometrical quality of cut. Optical microscopic images of top and bottom kerf widths with parametric settings as lamp current 180 Amp, pulse width at 2.3 ms, pulse frequency at 20 Hz, compressed air pressure at 8 kg/cm² and cutting speed at 100 mm/min are shown in Fig. 13 (a-b).

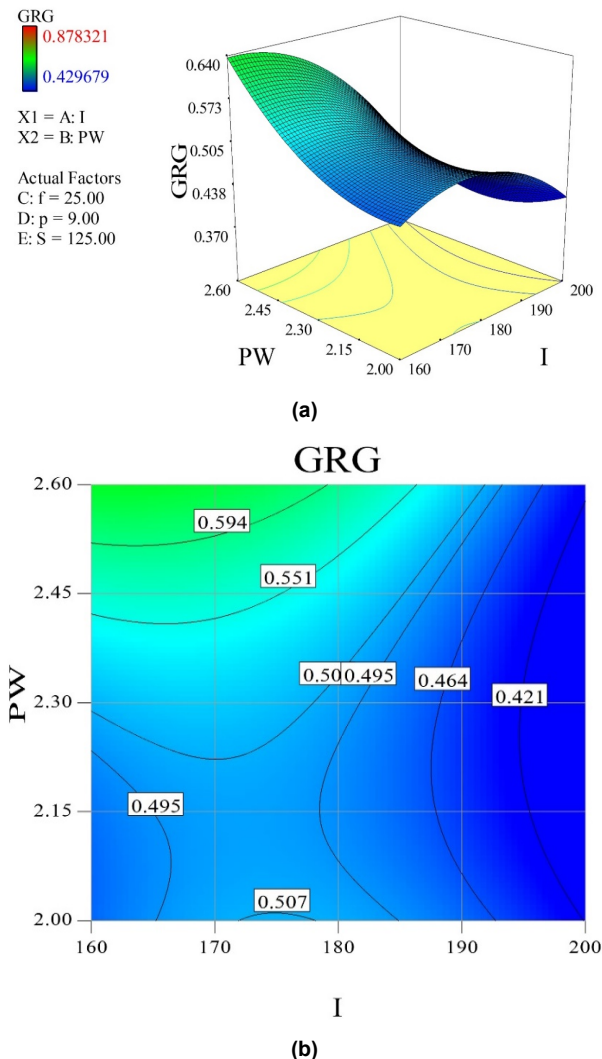


Figure 9. Combined effects of pulse width and lamp current on GRG: (a) response surface plot; (b) contour plot

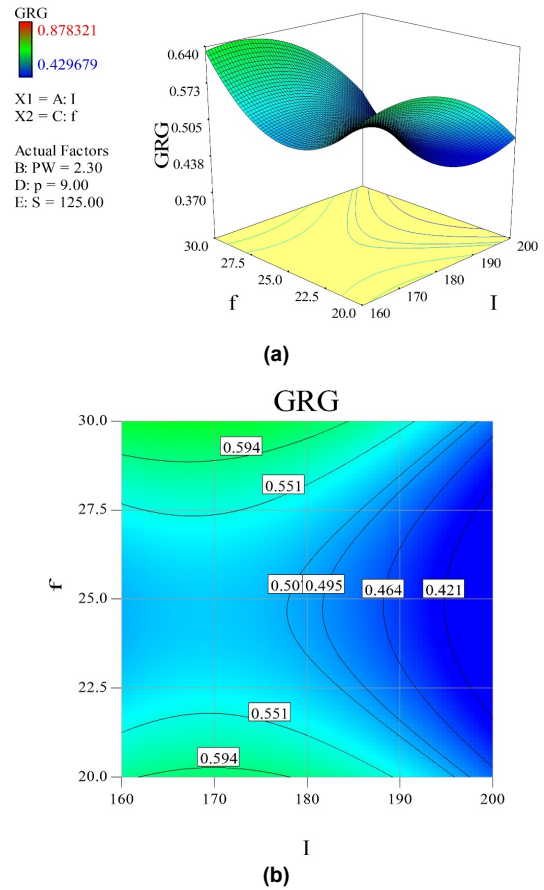


Figure 10. Combined effects of pulse frequency and lamp current on GRG: (a) response surface plot; (b) contour plot

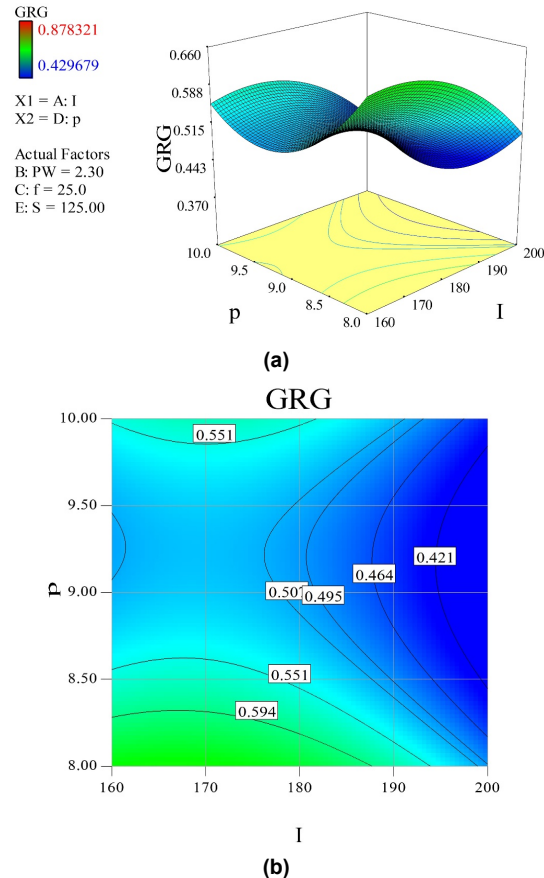
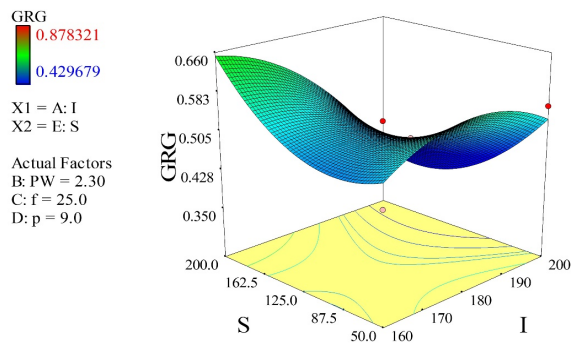
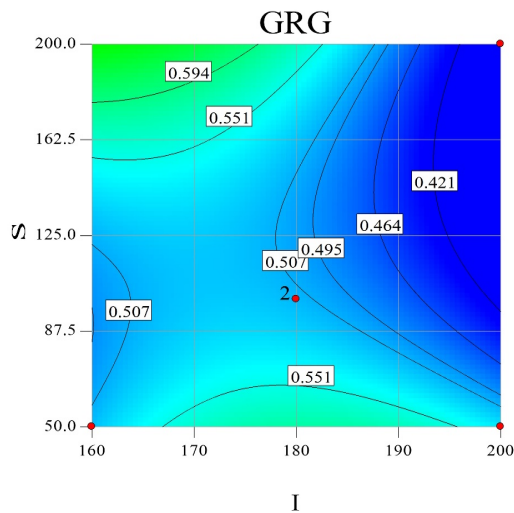


Figure 11. Combined effects of compressed air pressure and lamp current on GRG: (a) response surface plot; (b) contour plot



(a)



(b)

Figure 12. Combined effects of cutting speed and lamp current on GRG: (a) response surface plot; (b) contour plot

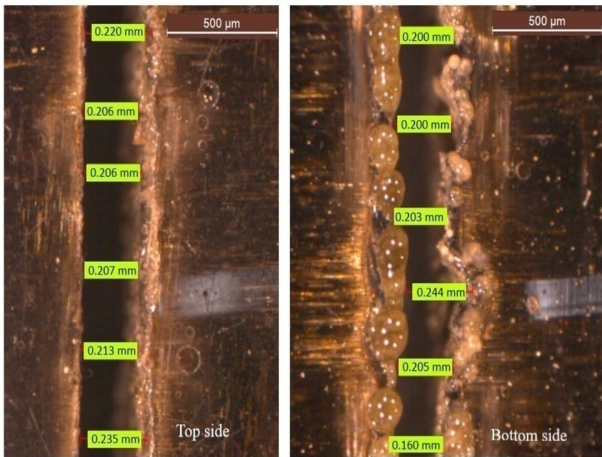
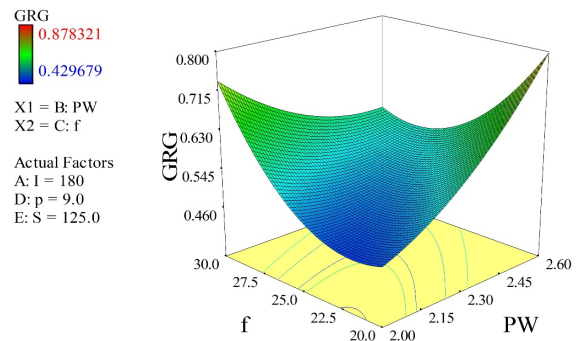
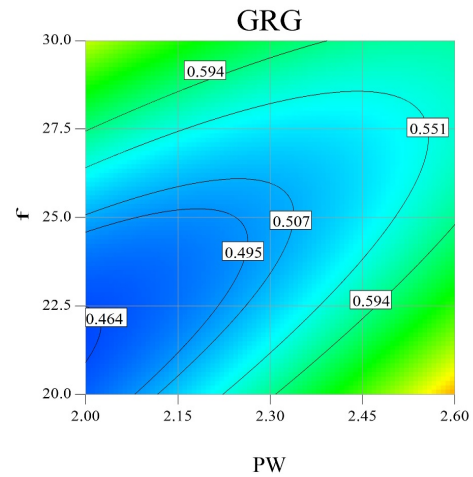


Figure 13. Optical microscopic image of kerf width (a) top side (b) bottom side at $I=180$ Amp, $PW=2.3$ ms, $f=20$ Hz, $p=8$ kg/cm², and $S=100$ mm/min

Figures 14-16 shows the combined effects of $PW-f$, $PW-p$ and $PW-S$ on the values of grey relational grades. By these graphs, it can be inferred that the higher values of pulse width (2.6 ms) are able to provide the higher values of grey relational grades for the satisfactory quality of multiple kerf characteristics. This is due to the fact that interaction time between the incident laser beam and the composite surface is increased at higher pulse width (2.6 ms) and affect kerf quality characteristics remarkably.

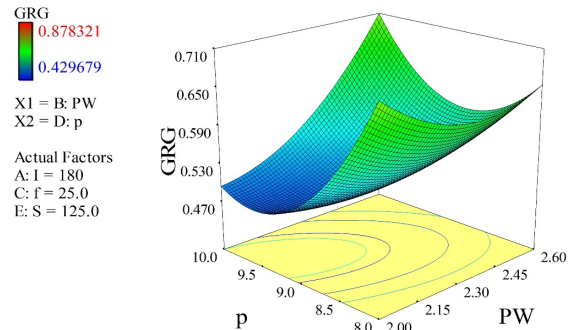


(a)

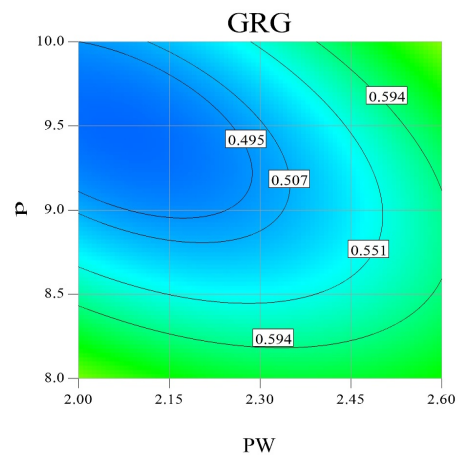


(b)

Figure 14. Combined effects of pulse frequency and pulse width on GRG: (a) response surface plot; (b) contour plot

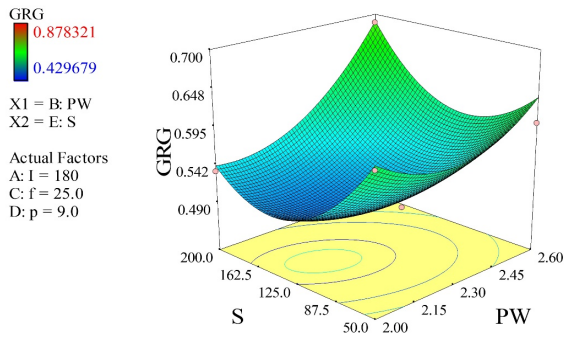


(a)

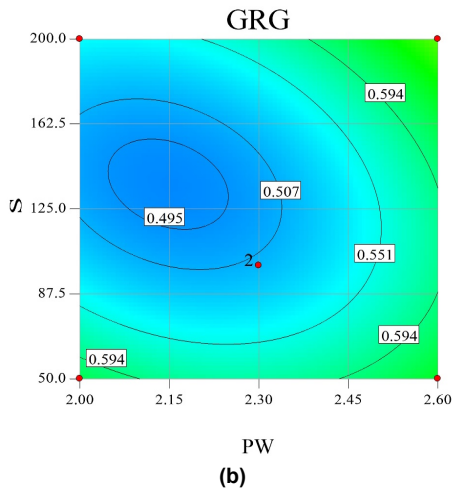


(b)

Figure 15. Combined effects of compressed air pressure and pulse width on GRG: (a) response surface plot; (b) contour plot

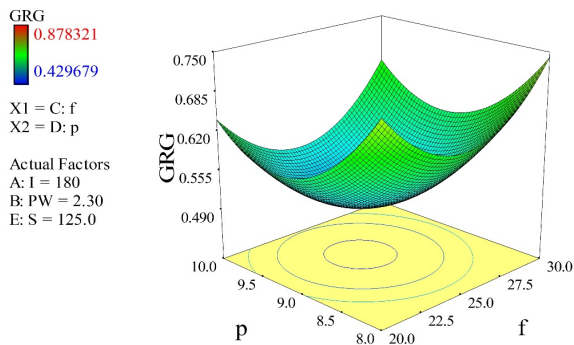


(a)

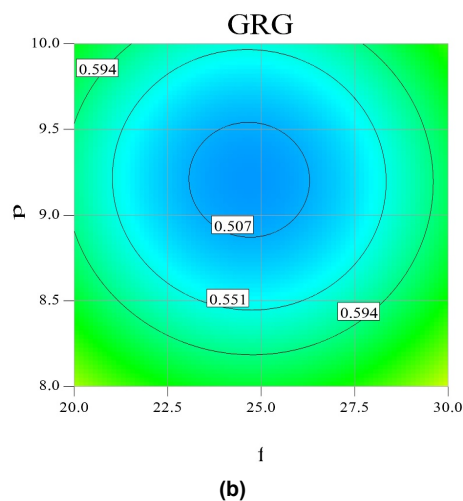


(b)

Figure 16. Combined effects of cutting speed and pulse width on GRG: (a) response surface plot; (b) contour plot



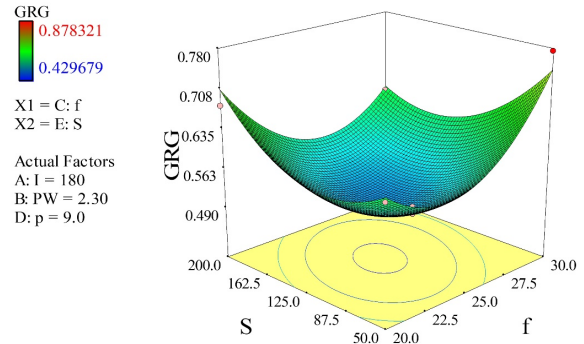
(a)



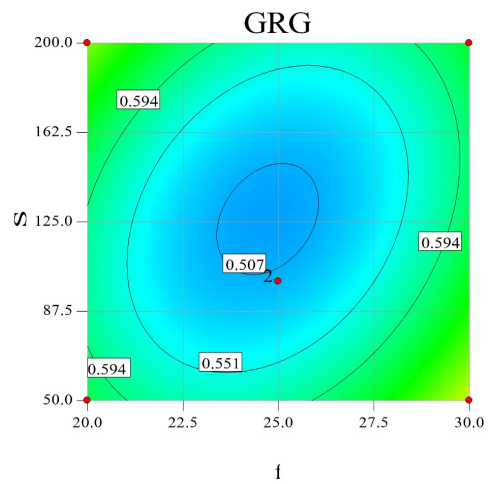
(b)

Figure 17. Combined effects of compressed air pressure and pulse frequency on GRG: (a) response surface plot; (b) contour plot

The combined effects of f - p and f - S on the values of grey relational grades are shown in Figure 17-18. These figures show that higher value of grey relational grades found at the higher setting of pulse frequency (30 Hz) with lower settings of compressed air pressure (8 kg/cm²) and cutting speed (50 mm/min). This may be due to that higher pulse frequency provides sufficient time to burn fibers and epoxy resin of BFRP composite laminates. Figure 19 (a-c) shows the optical microscopic images of kerf width at lower, moderate, and higher levels of pulse frequency. Moreover, a lower value of pulse frequency also increases the tendency of the fiber's disorderliness of burning.

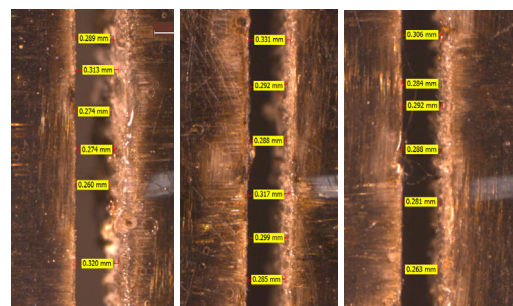


(a)



(b)

Figure 18. Combined effects of cutting speed and pulse frequency on GRG: (a) response surface plot; (b) contour plot



(a)

(b)

(c)

Figure 19. Optical microscopic images of kerf width at (a) lower, (b) moderate, and (c) higher pulse frequency

The combined effects of p - S on the value of grey relational grades are shown in Figure 20. It has been observed that with the increase in the values of

compressed air pressure and cutting speed, the values of grey relational grades decrease. It is a fact that higher compressed air pressure (10 kg/cm²) and cutting speed (200 mm/min) increase the quality of kerf characteristics because of their combined effects. These effects provide the continuous and fast removal of dross and burnt fibers from the kerf edges. It decreases the kerf deviation and improve the geometrical accuracy of the cut. Whereas in the present research, due to the higher burning point of basalt fiber (approx. 1500 °C), BFRP composite requires low cutting speed to the proper burning of fibers. Moreover, Basalt fiber also has a unique property to stop burn with the removal of the heat source. Besides, at the higher compressed air pressure (10 kg/cm²), possibilities for the occurrence of high-temperature oxidation reaction at the composite surface are also minimized.

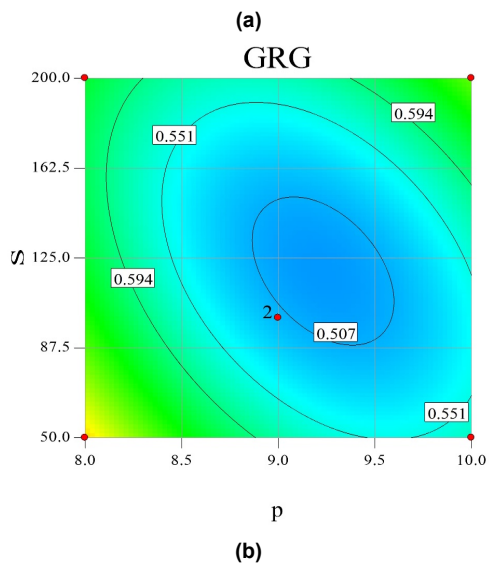
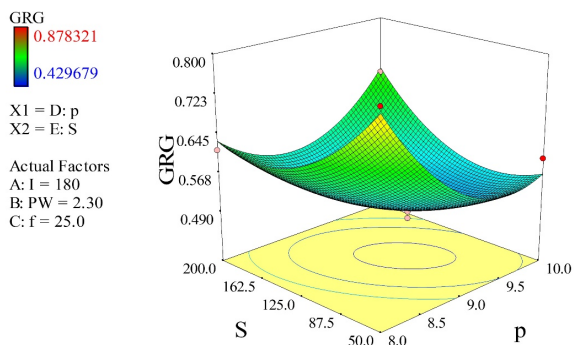


Figure 20. Combined effects of cutting speed and compressed air pressure on GRG: (a) response surface plot; (b) contour plot

During Nd:YAG laser cutting of BFRP composite, irregular shapes have been also observed at the bottom side of the cut. These shapes are formed due to the difference in thermal properties between basalt fiber and epoxy matrix. This is due the heat transfer by the fiber filaments to the polymer matrix. Epoxy has vicious nature, so when it melted, ejection is difficult and heat accumulation takes place at the bottom side of the cut and results in droplets deposition as shown in Fig. 21 (a-c). Figure 22 (a-b) shows the peeling off structure of basalt fibers at the top side of laser cut. This is due to the fact of the heat accumulated by the basalt fibers are sufficiently high to decompose polymer matrix without

burning of fibers. It is also shown in the SEM images of the cut edge surface in Fig. 23 (a-b). Moreover, it has been observed that heat conduction properties of basalt fiber and epoxy resin also responsible for improper laser cutting of BFRP composite.

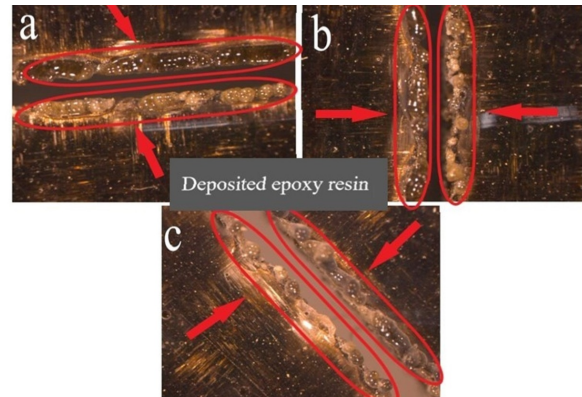


Figure 21 (a-c). Deposition of epoxy resin at bottom side of cut in different experimental trails

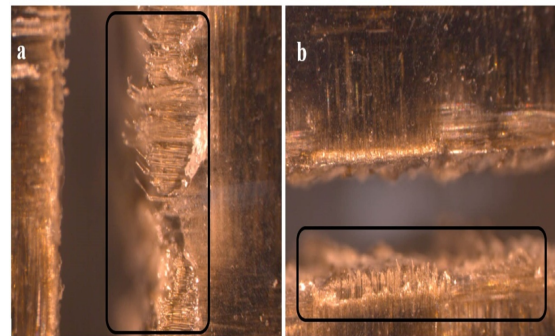


Figure 22 (a-b). Structure of fibers at the cut edge surface

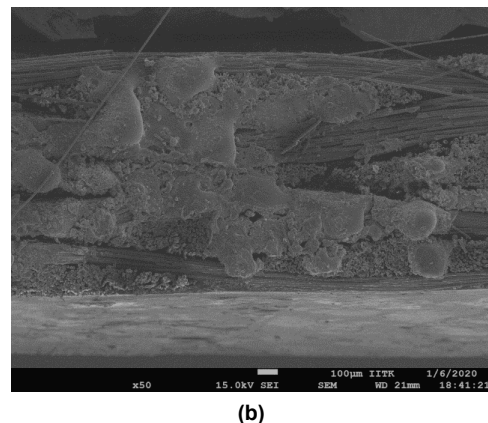
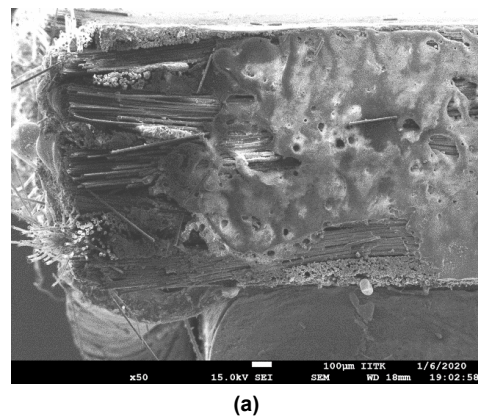


Figure 23 (a-b). SEM images showing the structure of fibers at the cut edge surface

5. CONCLUSION

In the present study, an attempt has been made to cut Basalt fiber reinforced polymer composite laminate by using a pulsed Nd-YAG laser system. To ascertain the better geometrical accuracy of the cut, major kerf quality characteristics such as top and bottom kerf widths, top and bottom kerf deviations and kerf taper have been simultaneously optimized by using a hybrid grey relational based genetic algorithm optimization approach. The aim of this research is to pave the way for geometrically accurate laser cutting of Basalt fiber reinforced polymer composites. The following conclusions have been drawn by the present research:

- In the present research, efficient cutting of 1.60 mm thick Basalt fiber reinforced polymer composite laminate by using pulsed Nd:YAG laser system have been attempted.
- The geometrical quality of the cut is quantified in the terms of top kerf width (TKW), bottom kerf width (BKW), top kerf deviation (TKD), bottom kerf deviation (BKD) and kerf taper (KT).
- A grey relation based genetic algorithm hybrid approach is employed to single index optimization of multiple kerf quality characteristics.
- The optimum settings of laser cutting parameters obtained by using GRA based multi-objective optimization are lamp current 180 Amp, pulse width 2.6 ms, pulse frequency 30 Hz, compressed air pressure 8 kg/cm² and cutting speed 50 mm/min.
- The optimal settings of cutting parameters obtained by GRGA are lamp current 184.5 Amp; pulse width 2 ms; pulse frequency 30 Hz, compressed air pressure 8 kg/cm² and cutting speed 50 mm/min.
- GRGA provides an overall improvement of 16.80 % as compared GRA in kerf quality characteristics at optimal parametric settings.
- Hybrid GRGA approach is better than GRA for predicting the optimal laser cutting parameters.
- From the analysis of results, lamp current has been found the most significant factor for all kerf quality characteristics followed by pulse width, compressed air pressure, pulse frequency and cutting speed in pulsed Nd:YAG laser cutting of BFRP composite laminates.
- The authors have confidence that the outcomes of this study will lead the researchers and modern industries to cut the FRP composite materials with higher accuracy and geometrical precision.

ACKNOWLEDGMENT

The authors are gratefully thankful to Dr. B.N. Upadhyay, SOF, Solid State Division Raja Ramanna Centre for Advanced Technology (RRCAT), Indore (M.P) India for the assistance of providing the experimental setup for the conduction of the experiments.

REFERENCES

[1] Lee S, Yop K, Park S. Influence of chemical surface treatment of basalt fibers on interlaminar shear strength and fracture toughness of epoxy-based composites. *Journal of industrial and engineering chemistry* 2015; 32; 153-156.

- [2] Wu Q, Chi K, Wu Y, Lee S. Mechanical, thermal expansion, and flammability properties of co-extruded wood polymer composites with basalt fiber reinforced shells. *Journal of Materials & Design* 2014; 60; 334-342.
- [3] Kishore SJ, Teja PC, Eshwariha B, Reddy KH. Experimental Control of Kerf Width Taper During Abrasive Water Jet Machining. *FME Transactions* 2019;47:585-90.
- [4] Mello MD. Laser cutting of non-metallic composites. *Laser processing: fundamentals, applications and systems engineering*. 1986: 668; 288-290.
- [5] Gautam GD, Pandey AK. Pulsed Nd:YAG laser beam drilling: A review. *Optics and Laser Technology*. 2018: 100; 183-215.
- [6] Lau WS, Lee WB, Pang SQ. Pulsed Nd:YAG laser cutting of carbon fibre composite materials. *Annals of the CIRP*. 1990: 39 (2); 179-182.
- [7] Ilio AD, Tagliaferri V. Cutting mechanism in drilling of aramid. *International journal of machine tools and manufacturing*. 1990: 31 (2); 155-165.
- [8] Mathew J, Goswami GL, Ramakrishnan N, Naik NK. Parametric studies on pulsed Nd:YAG laser cutting of carbon fibre reinforced plastic composites. *Journal of Materials Processing Technology*. 1999: 90; 198-203.
- [9] Negarestani R, Li L, Sezer HK, Whitehead D, Methven J. Nano-second pulsed DPSS Nd:YAG laser cutting of CFRP composites with mixed reactive and inert gases. *International Journal of Advance Manufacturing Technology*. 2010: 49: 553-566.
- [10] Leone C, Genna S. Heat affected zone extension in pulsed Nd:YAG laser cutting of CFRP. *Composites Part B*. 2018: 140: 174-182.
- [11] Cenna A, Mathew P. Analysis and prediction of laser cutting parameters of fibre reinforced plastics (FRP) composite materials. *International Journal of Machine Tools and Manufacturing*. 2002: 42; 105-113.
- [12] Gautam GD, Pandey AK. Teaching Learning Algorithm based Optimization of Kerf Deviations in Pulsed Nd:YAG Laser Cutting of Kevlar-29 Composite Laminates. *Infrared Physics and Technology*. 2017: 89; 203-217.
- [13] Gautam GD, Mishra, DR. Firefly algorithm based optimization of kerf quality characteristics in pulsed Nd:YAG laser cutting of basalt fiber reinforced composite. *Composites Part-B*. 2019: 176; 107340.
- [14] Gautam GD, Mishra, DR. Evaluation of Geometrical Quality Characteristics in Pulsed Nd:YAG Laser Cutting of Kevlar-29 / Basalt Fiber Reinforced Hybrid Composite Using Grey Relational Analysis Based on Genetic Algorithm. *FME Transactions*: 47 (3); 560-575.
- [15] Gautam GD, Mishra DR. Dimensional accuracy improvement by parametric optimization in pulsed Nd:YAG laser cutting of Kevlar-29/Basalt fiber reinforced hybrid composites. *Journal of the Brazilian Society of Mechanical Sciences and Engineering*. 2019: 41 (7); 1-22.

- [16] El-Taweel TA, Maaboud AM, Azzam BS, Mohammad AE. Parametric studies on the CO₂ laser cutting of Kevlar-49 composite. *International Journal of Advance Manufacturing Technology*. 2009; 40; 907-917.
- [17] Choudhury IA, Chuan PC. Experimental evaluation of laser cut quality of glass fibre reinforced plastic composite. *Optics and Lasers in Engineering*. 2013; 51; 1125-1132.
- [18] Kharwar PK, Verma RK. Grey Embedded in Artificial Neural Network (ANN) Based on Hybrid Optimization Approach in Machining of GFRP Epoxy Composites. *FME Transactions* 2019; 47 pp: 641-8.
- [19] Adalarasan R, Santhanakumar M, Rajmohan M. Optimization of laser cutting parameters for Al6061 /SiCp/Al₂O₃ composite using grey based response surface methodology. *Measurement*. 2015; 73; 596-606.
- [20] Rao R, Yadava V. Multi-objective optimization of Nd:YAG laser cutting of thin superalloy sheet using grey relational analysis with entropy measurement. *Optics and Laser Technology*. 2009; 41; 922-930.
- [21] Tamrin KF, Nukman Y, Choudhury IA, Shirley S. Multiple-objective optimization in precision laser cutting of different thermoplastics. *Optics and Lasers in Engineering*. 2015; 67; 57-65.
- [22] Mishra DR, Gautam GD, Prakash D, Bajaj A, Sharma A, Bist R, Gupta S. Optimization of Kerf Deviations in Pulsed Nd:YAG Laser Cutting of Hybrid Composite Laminate Using GRA. *FME Transactions*, 2020; 48 (1); 109-116.
- [23] Pandey AK, Gautam GD. Grey relational analysis-based genetic algorithm optimization of electrical discharge drilling of Nimonic-90 superalloy. *Journal of the Brazilian Society of Mechanical Sciences and Engineering* 2018; 40: 1-16.

NOMENCLATURE

f	Pulse frequency, in Hz
GC_{ij}	Grey relational coefficient for the i^{th} experiment and j^{th} response
I	Lamp current, in Amp
m	Number of responses
p	Air pressure, in kg/cm ²
PW	Pulse width, in ms
S	Cutting speed, in mm/min
t	Thickness of the composite laminate.
Y_i	i^{th} normalized value
Y_{ij}	i^{th} normalized value for j^{th} response
Y_{oj}	Ideal normalized value of j^{th} response
Z_{ij}	Normalized value for i^{th} experiment for j^{th} response
AFRP	Aramid fiber reinforced polymer
BFRP	Basalt Fiber Reinforced Polymer
BKD	Bottom kerf deviation
BKW	Bottom kerf width
CFRP	Carbon fiber reinforced plastic
FRP	Fiber reinforced polymer
GA	Genetic algorithm

GFRP	Glass fiber reinforced polymer
GRA	Grey relational analysis
GRC	Grey relational coefficients
GRG	Grey relational grade
GRGA	Grey relational analysis based genetic algorithm
HAZ	Heat affected zone
KD	Kerf deviation
KW	Kerf width
KT	Kerf taper
LBC	Laser beam cutting
LBM	Laser beam machining
Nd:YAG	Neodymium-doped yttrium aluminium garnet
RSM	Response surface methodology
TKD	Top kerf deviation
TKW	Top kerf width
TM	Taguchi methodology

Greek symbols

Δ	Absolute difference between Y_{oj} and Y_{ij}
Δ_{min} and Δ_{max}	The minimum and maximum values of Δ
λ	Distinguishing coefficient

ОПТИМИЗАЦИЈА КАРАКТЕРИСТИКА КВАЛИТЕТА РЕЗА КОД РЕЗАЊА ЛАСЕРОМ BFRP КОМПОЗИТА КОРИШЋЕЊЕМ ГЕНЕТСКОГ АЛГОРИТМА БАЗИРАНОГ НА ГРЕЈ РЕЛАЦИОНОЈ АНАЛИЗИ

Г.Д. Гаутам, Д.Р. Мишра

Код машинске обраде ласером геометријски прецизно резање FRP композита представља задатак пун изазова пошто треба направити што квалитетнији рез. Циљ истраживања је да се одреде оптималне вредности параметара резања да би се добио геометријски прецизан рез код BFRP композитног ламината дебљине 1,60 мм. Експерименти су изведени применом пулног Nd:YAG ласера са напајањем од 250 W. Извор светла, ширина импулса, фреквенција импулса, притисак компримованог ваздуха и брзина резања су варирано да би се процениле различите карактеристике квалитета реза: ширина горњег и доњег дела реза, одступање горњег и доњег дела реза и сужење реза. Резултати експеримента су искоришћени за издвајање индекса оптимизације већег броја карактеристика квалитетног реза. Генетски алгоритам и греј релациона анализа су искоришћени у поступку оптимизације. Утврђене су оптималне вредности параметара резања: умерено напајање извора светла (184,5 Амп), мања ширина импулса (2 ms), притисак компримованог ваздуха (8 kg/cm²), брзина резања (50 mm/min) и већа фреквенција импулса (30 Hz). Конфирматорни експерименти су потврдили да оптималне вредности параметара резања могу да побољшају горњи део ширине реза, доњи део, одступања код горњег дела реза, одступања код доњег дела и сужења реза за 13,33%, 13,29%, 23,52%, 23,07% и 10,83%. Резултати експеримента су такође потврдили да је напајање извора светла најважнији параметар за све карактеристике квалитета реза.